Time-Resolved Surface Temperature Measurement of MALDI Matrices under Pulsed UV Laser Irradiation

ARTICLE *in* THE JOURNAL OF PHYSICAL CHEMISTRY A · APRIL 2004

Impact Factor: 2.69 · DOI: 10.1021/jp037811k

4 AUTHORS, INCLUDING:

Vladimir Frankevich
Research Center for Obstetrics, Gynecology a…
53 PUBLICATIONS **1,269** CITATIONS
SEE PROFILE

Juan Zhang
Novartis Institutes for BioMedical Research
17 PUBLICATIONS **537** CITATIONS
SEE PROFILE

Renato Zenobi
ETH Zurich
456 PUBLICATIONS **13,055** CITATIONS
SEE PROFILE

Time-Resolved Surface Temperature Measurement of MALDI Matrices under Pulsed UV Laser Irradiation

Antonis Koubenakis,† Vladimir Frankevich, Juan Zhang, and Renato Zenobi*

Department of Chemistry and Applied Biosciences, Swiss Federal Institute of Technology (ETH), ETH-Hönggerberg, CH-8093 Zürich, Switzerland

Received: December 11, 2003; In Final Form: February 16, 2004

Time-resolved examination of the surface temperature was performed for various MALDI matrices, irradiated by UV ($\lambda = 355$ nm, $\tau = 5$ ns) laser pulses. The temperature was measured by detecting the emitted blackbody radiation from the sample surface. The maximum surface temperature was observed to occur during the falling edge of the laser pulse, with a delay of 2 ns with respect to the laser pulse peak. Its value was found to depend on the kind of the matrix, the thickness of the sample and the laser fluence. For 2,5-dihydroxybenzoic acid, the most popular matrix, the peak temperature was found to be ∼850 and 1100 K at the lower (10 J/m^2) and the higher (100 J/m^2) fluences, respectively, used in this work.

Introduction

When irradiating organic crystals with UV laser pulses, electronically excited molecules exchange vibrational energy and/or transfer it to the surrounding medium with a half-life on the order of picoseconds.[1] The deposited thermal energy causes an increase of the solid temperature. On the basis of fluorescence measurements on matrix-assisted laser desorption ionization (MALDI) matrices,[2] it has been reported that a large percentage of the initially absorbed UV laser energy (∼80%) is converted to thermal energy. The lifetime of this process has been estimated to be 0.5−1 ns.[3] Because of the low thermal conductivity of organic solids, large temperature changes may be attained in the solid for nanosecond laser pulses that are usually employed in the MALDI. A high temperature of the system may play a key role for various processes that take place after the absorption of the laser energy in MALDI.

It has been argued on the basis of experiments and molecular dynamics (MD) simulations that the temperature increase during laser irradiation is important for the mechanisms of molecular ejection in MALDI. Depending on the rate of the temperature change in the solid, the ejection/desorption can be characterized as either a thermal surface vaporization[4] or a phase explosion.[5] Furthermore, the temperature increase can also affect the thermal degradation and the conformation of the biomolecules inside clusters of the ejected material.[6] Finally, ion formation in MALDI can be influenced in part by the temperature increase. Theoretical calculations predict that the probability of ion formation through thermoionization paths can become significant as the matrix temperature increases to 2000 K.[7,8]

Despite the importance of the issue, there has not been any experimental study of the time evolution of the matrix surface temperature, during and after the laser irradiation. Such information can be useful especially for the theoretical models and MD simulations as well as for interpretation of some of the mass spectrometry results. In this work, we report the time-resolved measurement of the surface temperature of two well-known MALDI matrices, 2,5-dihydroxybenzoic acid (2,5-DHB) and nicotinic acid (NA), during the irradiation with UV ($\lambda = 355$ nm, $\tau = 5$ ns) laser pulses at various fluences. The dependence of the peak surface temperature on sample thickness was also examined for 2,5-DHB, NA, 2-(4-hydroxyphenylazo)-benzoic acid (HABA), 2,4,6-trihydroxyacetophenone (THAP), dithranol, and ferulic acid. The experiments are based on the detection of the blackbody radiation emitted by the matrix surface at elevated temperature. Previous works on metal substrates[9,10] have shown that blackbody radiation emitted from hot irradiated surfaces can be used for a noncontact, fast (nanosecond time scale) detection of the temperature during and after the laser irradiation pulse.

Experimental Section

The apparatus used for this experiment is shown schematically in Figure 1. The samples are irradiated by a Nd:YAG (Minilite, Continuum, CA/USA) laser beam ($\lambda = 355$ nm, full width at half maximum (fwhm) = 5 ns). The pulse duration of the laser beam was measured using a high-speed silicon PIN photodiode (DET200, ThorLabs, NJ/USA) with a rise/fall time ≤ 1 ns and a digital oscilloscope (9350C, Lecroy, Switzerland) with a bandwidth of 500 MHz (2-ns time resolution). The laser beam is gently focused onto the sample surface to a spot size of about 3 mm × 1 mm. The laser fluence was varied using attenuators and/or filters. The values of the laser fluences ranged from 10 to 100 J/m^2. The reported values are uncorrected for scattering/reflection losses at the sample surface. All experiments are performed at fixed angles of incidence (45°) and detection (0°), with respect to the surface normal of the sample. The initial temperature of the sample was at approximately 300 K (room temperature). All experiments were performed at atmospheric pressure ($p = 1$ atm); i.e., the results may relate to atmospheric pressure MALDI more directly than to MALDI experiments carried out in a vacuum.

The blackbody radiation emitted from the sample surface was detected by a fast infrared InGaAs−PIN photodiode (model G8376−03, Hamamatsu, Herrsching, Germany) with a spectral response range of ∼0.9−1.7 μm. The detector's responsivity

* Author to whom correspondence may be addressed. E-mail: zenobi@org.chem.ethz.ch.

† Current address: Hellenic Air Force, 115 ΠΜ Akrotiri, Chania, Crete/Greece.

10.1021/jp037811k CCC: $27.50
Published on Web 03/09/2004

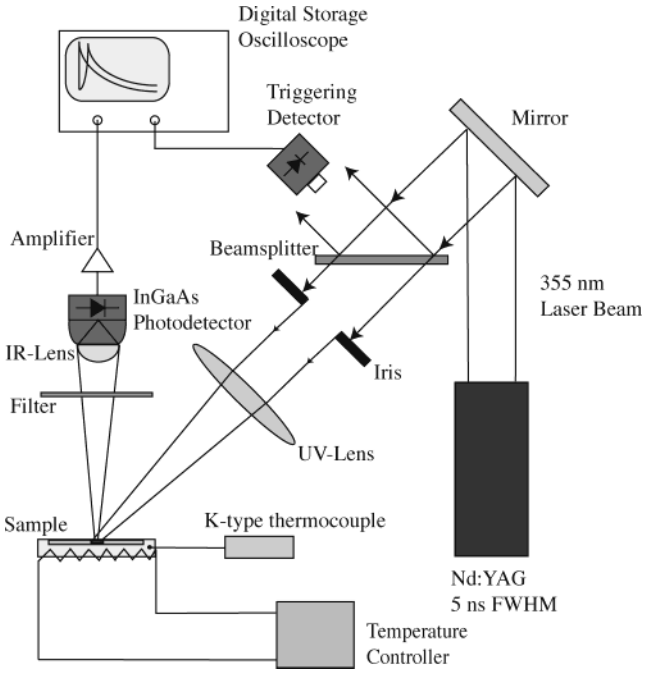

Figure 1. Schematic diagram of the experimental setup used to measure the surface temperature.

was 0.95 A/W at 1.55 μm. An operational amplifier (Burr-Brown, OPA658, 900 MHz) is used for amplifying the signals giving a 310 V/A output. The rise/fall time of the amplifier and electronic circuitry was determined separately, resulting in an overall (detector + amplifier) response time of 2 ns. The signals were recorded on the oscilloscope and transferred to a computer for storage and data processing. All the presented data are unsmoothed. Because the detector is not sensitive to temperatures lower than 550−600 K, some points that gave negative voltage readings were removed as they have no physical meaning. Normally 100 laser shots were averaged in each recorded blackbody spectrum. However, in the case of the thin samples, more than 100 laser shots were utilized because of the lower S/N ratio. An infrared lens (5 mm ∅) with a focal length of 3.2 mm attached to the input window of the detector was used to image a spot of 0.9 mm diameter in the center area of the laser irradiated surface, onto the active area of the detector (0.3 mm ∅) in a 3:1 transfer ratio. Care was taken to keep the imaged part of the surface in the detector active area smaller than the laser heated area. The acceptance angle is limited to 28°, corresponding to an F-number of 0.5. The total detection solid angle of the system was ∼0.2 sr. An optical cutoff 850-nm filter (model FSR-RG850, 25.4 mm ∅, Newport Instruments, Switzerland) was used to protect the infrared detector from scattered radiation (laser light and fluorescence from the sample). Although the optical detection setup (lens and infrared detector) is insensitive to radiation < 1 μm, the output signal was found to be influenced by the presence of some scattered/reflection radiation when the cutoff filter was not used.

All sample targets were prepared using the standard "dried droplet" method on a polished stainless steel substrate, which resulted in many small crystallites on the substrate surface. Because of the well-known inhomogeneity of microcrystalline MALDI preparations,[11] we measured both samples with thin (usual amount) and thick coverage. We refer to "thin" sample layers when the metal substrate is only partially covered by sample crystallites and to "thick" sample layers for cases where the substrate is completely covered by the sample. However, in either case, it is not possible to provide an exact number for the sample thickness, because of the heterogeneous nature of the MALDI samples. In the thin-layer preparation, the droplet on the metal substrate was spread, to avoid buildup of a thick crystal layer, and subsequently allowed to dry at room temperature. In the case of "thick" samples, we used depositions with a thickness of several hundreds of micrometers up to a millimeter, to ensure that the metal substrate is not visible to the laser irradiation. All the matrix compounds were obtained from Fluka (Buchs, Switzerland).

Results and Discussion

For converting the infrared photodiode signals to temperature values, a calibration is needed. The straightforward procedure proposed for metal surfaces[9,10] cannot be applied here. The reason is that metallic samples can easily be held at a constant, elevated temperature while the signal from the emitted radiation is recorded. In the case of MALDI matrices, a prolonged temperature increase above ∼500 K would cause sublimation or melting of the sample. The sublimation temperature for MALDI matrices is in the range of ∼350−500 K.[12] Methods for determining the emissivity, e.g., based on the measurement of the reflection and/or the transmission,[9] cannot be applied either because of the roughness of the matrices' surface and the presence of the metal substrate. Therefore a different procedure was followed in order to convert our signals to temperature. Initially, the whole optical setup was calibrated using a stainless steel substrate that has a known emissivity. The bulk temperature of the stainless steel was controlled by a resistance heater and measured by a K-type thermocouple attached to it. Figure 2a depicts the infrared photodiode signal output (data points) recorded for various temperatures of the stainless steel surface. The output signal V (data in Figure 2) is proportional to T^n where $n > 4$ and T is the temperature of the sample.[13] Therefore if T_B is the equivalent blackbody temperature, we have: $V \propto \epsilon_{ss} T_{ss}^n = T_B^n$, where ϵ_{ss} ($\epsilon_{ss} \approx 0.20$) is the emissivity of the polished stainless steel[14] and T_{ss} the measured substrate temperature by thermocouple. The slope n (12.4) was determined by fitting the data in a log−log plot as shown in the inset of Figure 2a. Such a high power for the temperature scaling was expected because only a narrow spectral interval of the blackbody spectrum is sensed. In previous studies with an infrared radiation pyrometer, n has been found to be as high to 12.[13] At a detector voltage V corresponding to a temperature T_{ss} determined by the calibration, the matrix temperature can be obtained in an analogous fashion by the following equation[13]

$$T_{matrix} = (\epsilon_{ss}/\epsilon_{matrix})^{1/n} T_{ss} \quad (1)$$

where ϵ_{matrix} is the emissivity of the matrix. The ϵ_{matrix} value was estimated from literature reports to be ∼0.90 in the range of 1−2 μm and at temperatures higher than 475 K. This estimation was based on studies of polymers[15] and on the fact that for nonmetallic materials the emissivity is much higher than that of metals. In general, the spectral emissivity of nonmetallic substrates has a weak dependence on wavelength, especially in the infrared. The emissivity is nearly independent of angles from 0 up to 50 degrees, and the temperature dependence is weak. Finally, since emission and reflection processes involve layers well into the surface, surface conditions such as roughness are not likely to significantly influence the emissivity.[16] The same ϵ_{matrix} was assumed for all the matrix compounds examined. Figure 2b shows how the photodiode signal V (in mV) can be converted into a matrix temperature T_{matrix} (K) using eq 1, based

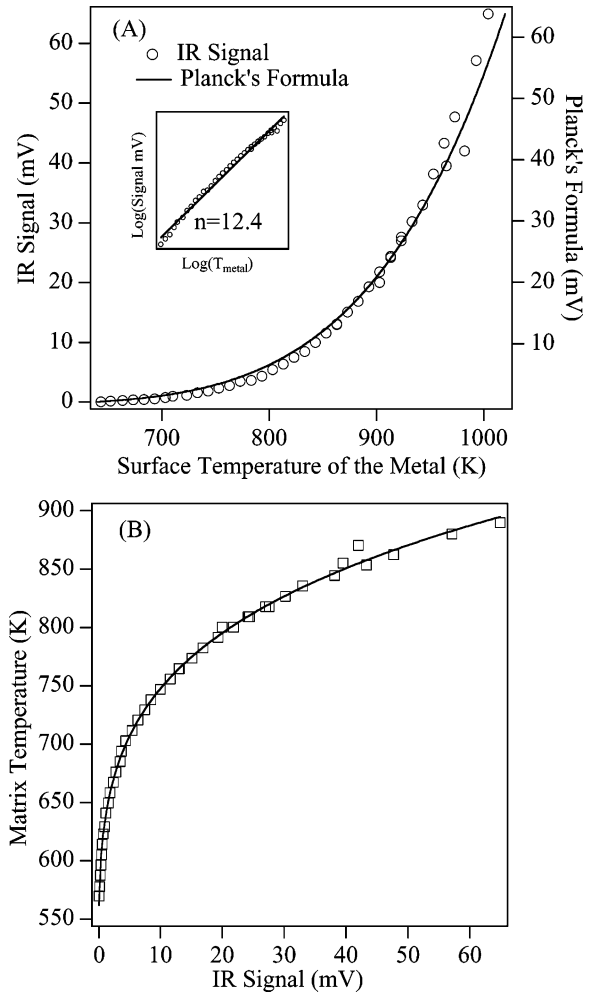

Figure 2. (a) Static calibration of the IR photodiode detector for different surface temperatures (○) of stainless steel. The full line represents the signal predicted by eq 2 based on Planck's law. Inset, see text. (b) Data converted to allow the determination of the matrix temperature.

on the calibration shown in Figure 2a. The solid line in Figure 2b is a fit which was employed for this, including extrapolations beyond the temperature range used in the calibration.

Finally, to ensure that the metal substrate emissivity is independent of temperature or angle in the wavelength range of 1−2 μm, we calculated the expected output signal as a function of temperature from the blackbody theory using a constant value of emissivity. This estimation, shown as a solid line in Figure 2a, was based on the parameters of our setup given below and on Planck's law (blackbody radiation). The thermal emission signal collected by the detector can be expressed in general[9,17] by

$$S(T) = \frac{R_\Omega A}{\pi} G_{\text{Phot}} G_{\text{opAmp}} TR \int_{\lambda 2}^{\lambda 1} \int_{\phi 2}^{\phi 1} \int_{\theta 2}^{\theta 1} \epsilon(\lambda,\phi,\theta,T)) \times J_{BB,\lambda}(\lambda,T)\, \mathrm{d}\theta\, \mathrm{d}\phi\, \mathrm{d}\lambda \quad (2)$$

where T is the temperature, θ and ϕ are the polar and azimuthal angles, λ is the wavelength (∼1−2 μm), R_Ω (50 Ω) is the impedance of the oscilloscope, A is the area on the sample (7.8 × 10^{-1} mm^2) that is seen by the detector, TR (1) is the spectral transmittance of the optical path (filter, lens), G_{Phot} (0.95 V/W) is the response factor of the InGaAs detector, G_{opAmp} (310 V/A) is the gain of the operational amplifier, and $J_{\text{BB},\lambda}$ is the blackbody emissive power which follows Planck's radiation law,[18] $J_{\text{BB},\lambda}$ = $2\pi C_1/[\lambda^5 \exp(C_2/\lambda T) - 1]$, where C_1 (3.7420 × 10^8 W μm^4/m^2) and C_2 (1.4388 × 10^8 K μm) are constants. We have assumed a constant emissivity for stainless steel, (ϵ = 0.20 at T = 300 K, λ = 2 μm). As shown in Figure 2a, the theoretical estimate (line) is in excellent agreement with the experimental data points, showing that a constant emissivity of the metal for the given temperature and the wavelength range can be used, i.e., that eq 1 can be applied with ϵ_{ss} = 0.20.

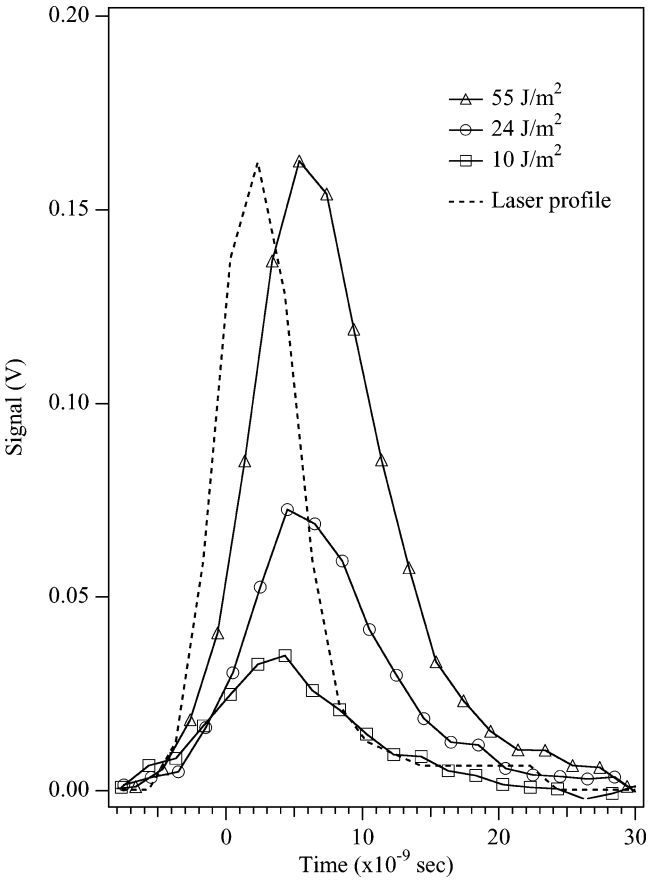

Figure 3. Nd:YAG laser pulse profile and typical thermal emission signals from the irradiation of thick films of 2,5-dihydroxybenzoic acid at various laser fluences. The spectra were recorded at 10 mJ/cm^2, 24, and 55 J/m^2, and each of them was averaged over 100 laser pulses.

We first examine the dependence of the surface temperature of 2,5-DHB and nicotinic acid matrices as a function of laser fluence when irradiating thick samples of the compounds. Typical blackbody emission signals when irradiating 2,5-DHB with various laser fluences are shown in Figure 3, along with the laser pulse profile. Such curves were recorded for all the matrices examined. For all fluences, the shape and the height of the curves are found to remain constant over a large number of irradiation pulses (>300). As can be seen in the figure, the maximum signal occurs during the falling edge of the laser pulse. This was found for all fluences examined. The time delay of the peak signal with respect to the peak intensity of the laser was found to be 3 ns. Taking into account that the time resolution of our apparatus is 2 ns, the delay may be even shorter, but if true, it is not possible to resolve it using the present setup. In general, the detected curves were found to have a fwhm of ∼10−12 ns, and the peak of the detection signal was found to increase with increasing laser fluence.

Parts a and b of Figure 4 show the temperatures transients for different laser fluences for 2,5-DHB and nicotinic acid, respectively. The temperature is obtained from the signals using the calibration procedure described above. For 2,5-DHB, the

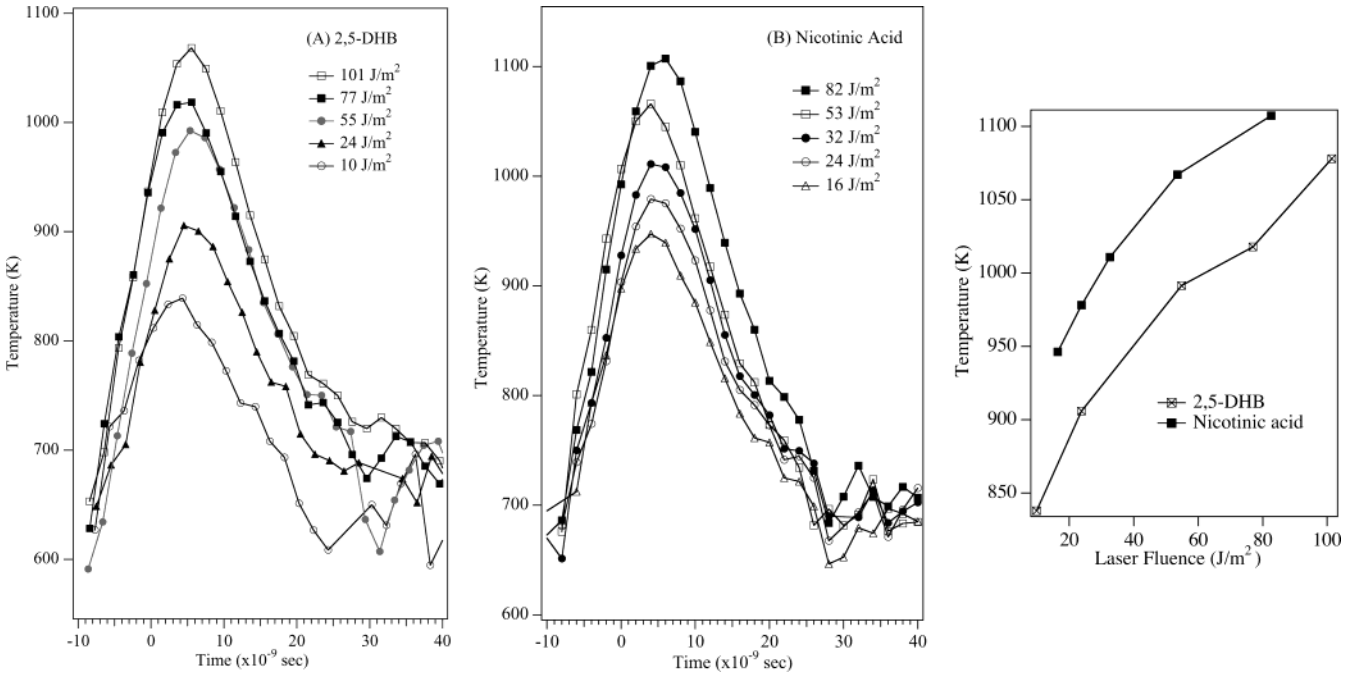

Figure 4. (a) Transient temperature profiles at different laser fluences recorded for irradiation of thick films of 2,5-dihydroxybenzoic acid at various laser fluences. (b) Transient temperature profiles at different laser fluences recorded for irradiation of thick films of nicotinic acid at various laser fluences. (c) Dependence of the peak temperature on laser fluence. Because of the nonlinear shape of the calibration curve, the uncertainty is estimated to be ±100 K in the low-temperature regime (<650 K), dropping to ±20 K in the high-temperature regime.

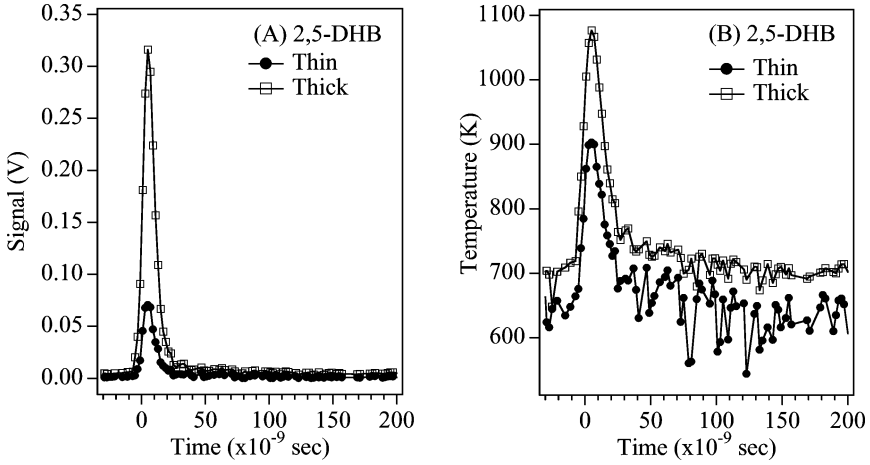

Figure 5. Time-resolved temperature measurements of thin and thick films of DHB irradiated with 355-nm, 100-J/m^2 laser pulses. (a) Detector output signals and (b) conversion to temperature.

peak temperature was found to range from 830 K to almost 1080 K depending on the laser fluence. Afterward the temperature drops to ∼700−650 K in 30 ns. The fluence dependence of the temperature for nicotinic acid is shown in Figure 4b. These experiments were done under conditions identical to that of 2,5-DHB. In general, the temperature profiles are similar to those observed for 2,5-DHB. However, the temperature decrease is faster (∼20 ns) than for 2,5-DHB. Another difference is in the temperature maximum observed for different laser fluences. As shown in Figure 4c, peak temperatures reached in the case of nicotinic acid were higher than those for 2,5-DHB for all fluences examined. On the other hand, the dependence of peak temperatures on laser fluence was found to be very similar for both matrices: initially, the temperature increases linearly, but at higher fluences (∼100 J/m^2), it appears to show a sublinear trend. This behavior at higher fluences will be discussed below.

We next examine the time-resolved measurements of the surface temperature when irradiating thin and thick samples of various MALDI matrices. Measurements were performed on 2,5-DHB, nicotinic acid, HABA, dithranol, ferulic acid, and THAP at a laser fluence of ∼100 J/m^2. Figure 5 depicts the recorded signals (part a) and the transient surface temperature curves (part b) for thin and thick samples of 2,5-DHB. Some interesting features were observed. First, as shown in the graph, the peak temperature for the thick 2,5-DHB (∼1080 K) was found to be larger than that of the thin sample (∼900 K). Second, the drop of the temperature is steeper in the case of the thick sample as the temperature drops by more than 300 K in a time period of 15 ns. In contrast, for the same time interval, a decrease of 200 K is observed for the thin samples. Similar observations were made for all the matrices examined. Table 1 summarizes the results from the various matrices for thin and thick samples irradiated by ∼100 J/m^2 laser pulses. The peak temperatures of the recorded curves are reported in Table 1. In all cases, the peak temperatures for the thick samples were larger than the ones found for thin samples.

TABLE 1: Peak Temperatures (K) Obtained after Irradiation of Various MALDI Matrices with 100-J/m^2 Laser Pulses

sample	DHB	nicotinic acid	HABA	THAP	dithranol	ferulic acid
thin	920	930	900	925	820	750
thick	1090	1120	1130	1030	1090	1130

Considering first the temperature curves observed for the various matrices, a temperature maximum very soon after the laser pulse is in agreement with what has been found in fluorescence measurements of these compounds.[2] Most of the absorbed energy (80%) is expected to be converted to thermal energy, increasing the temperature within 0.6−1 ns. On the other hand, the fast surface cooling that is observed after the laser pulse can be attributed to different processes. Three mechanisms can be responsible for the surface temperature drop, namely, heat diffusion, surface vaporization, and thermal emission. Energy loss via thermal emission is very minor if at all present. The total thermal emission power was calculated to be ∼0.16 W at 1100 K. The heat diffusivity for molecular solids is typically in the range of $D \approx 10^{-7}$ m^2/s, and the dissipation time of the thermal energy by thermal conduction is ∼1 μs. Compared to the 5-ns width of the laser pulse, the thermal energy remains mainly in the irradiation volume (a situation referred to as "thermal confinement") for times up to 1 μs after the laser pulse. Thus, no significant loss of thermal energy from the surface of the sample is expected by this channel. On the other hand, cooling as a result of surface vaporization can be significant for surface temperatures exceeding the sublimation temperature of the matrix. Most of the matrices used in this study have sublimation temperatures in the range of 450−580 K. This means that vaporization will in every case become important during or shortly after the laser pulse, when the surface temperature has risen above the sublimation point of the compound. As a result, the peak temperature will depend on the surface vaporization and the sublimation temperature of the compound in addition to the absorption characteristics of the matrix and the laser fluence. This can be seen in the comparison of 2,5-DHB with NA (Figure 4c). Although 2,5-DHB is a much stronger absorber at 355 nm than nicotinic acid, the sublimation point of 2,5-DHB (478 K) is lower than that of nicotinic acid (573 K). This can explain the higher peak temperatures for NA observed at all fluences examined.

We next consider the dependence of the peak temperature on laser fluence. In mass spectrometry studies, the dependence of the desorption yield from 2,5-DHB on laser fluence has been examined for irradiation with UV laser pulses.[4] A quasithermal sublimation/desorption model was found to describe the desorption yields of the molecules. The model was based on the assumption that at low and moderate fluences (<100 J/m^2) a one-photon absorption process predominates, which is highly probable also from fluorescence measurements.[2,3,19] The surface temperature rise can be estimated from the equation

$$T = T_o + \frac{\alpha F_{LASER}}{\rho C_P} \qquad (3)$$

where T_o represents the initial temperature of the system, α (m^{-1}) the optical absorption coefficient, ρ (mol m^{-3}) the solid density, C_P (J mol^{-1} K^{-1}) the heat capacity of the system, and F_{LASER} (J m^{-2}) the laser fluence. Accordingly, the temperature change is expected to vary linearly with laser fluence, $\Delta T \propto F_{LASER}$. This analysis agrees with our observations for 2,5-DHB and NA, as the temperature was found to vary almost linearly with fluence (see Figure 4c), at least for moderate values of the laser fluence (10−60 J/m^2). On the other hand, absolute values for the peak temperatures cannot be derived from the equation to compare with the experimental observations, because there are additional parameters (surface vaporization) that must be taken into account and that affect the final peak temperatures. At higher fluences (>60 J/m^2), some deviation from linearity was found. The principal reason for this is certainly the increased vaporization rate at elevated temperature, which is not taken into account by eq 3. In addition, a high temperature in the molecular solid of the matrices can result in a metastable thermodynamic condition characterized by the occurrence of cavitation, bubbles, etc. in the irradiated volume.[5,20] At the highest fluences where the temperature of the solid is almost twice the melting point of the compounds, such a situation can also lead to a deviation from the linear behavior predicted by eq 3.

Finally, we consider the origin of the different peak temperatures observed for thin and thick samples of the various matrices. As seen in Table 1, the peak temperature of the thick sample was found to be higher than that of the thin one for all cases. As discussed above, surface vaporization is the most important process that affects the final surface temperature of the thick samples. The most reasonable explanation is that, for thin samples, an additional dissipation channel becomes important, i.e., heat diffusion into the metallic substrate. In the case of a thin matrix layer, fairly large metallic areas are exposed between the matrix crystallites. As the metal substrate has a much larger heat conductivity compared to the matrix, energy loss by thermal conduction into the metal becomes important, explaining the lower temperatures in the thin matrix samples as compared to the thick samples. It is possible that the matrix/metal system has a reduced emissivity, resulting from a sample thickness that is small compared to the (near) IR absorption depth and low effective area covered by the matrix. However, calculations with $\epsilon = 0.5$ showed that this only results in a lowering of the maximum temperature by about 20 K, i.e., a variation in the emissivity alone cannot account for the observed ∼200 K difference in temperature.

Conclusions

In summary, time-resolved measurements of the surface temperature were performed for various MALDI matrices, under irradiation by UV ($\lambda = 355$ nm, $\tau = 5$ ns) laser pulses. The temperature was probed by detecting the emitted blackbody radiation from the sample surface. A similar behavior of the temperature transients was found for all matrices examined. For 2,5-DHB and nicotinic acid, the peak surface temperature was found to range between ∼850 and 1100 K, depending on the thickness of the sample and the laser fluence. Evaporative cooling appears to be operative for all matrices studied, during the laser pulse or shortly after its onset, and largely controls the peak temperatures reached.

Acknowledgment. The authors would like to thank Mr. Heinz Benz for technical assistance.

References and Notes

(1) Hochstrasser, R. M. *Rev. Mod. Phys.* **1962**, *34*, 531.

(2) Ehring, H.; Sundqvist, B. U. R. *J. Mass Spectrom.* **1995**, *30*, 1303.

(3) Allwood, D. A.; Dyer, P. E.; Dreyfus, R. W. *Rapid Commun. Mass Spectrom.* **1997**, *11*, 499.

(4) Dreisewerd, K.; Schürenberg, M.; Karas, M.; Hillenkamp, F. *Int. J. Mass Spectrom. Ion Processes* **1995**, *141*, 127.
(5) Zhigilei, L. V.; Leveugle, E.; Garrison, B. J.; Yingling, Y. G.; Zeifman, M. I. *Chem. Rev.* **2003**, *103*, 321.
(6) Sadheghi, M.; Wu, X.; Vertes, A. *J. Phys. Chem. B* **2001**, *105*, 2578.
(7) Allwood, D. A.; Dreyfus, R. W.; Perera, I. K.; Dyer, P. E. *Rapid Commun. Mass Spectrom.* **1996**, *10*, 1575.
(8) Allwood, D. A.; Dyer, P. E.; Dreyfus, R. W.; Perera, I. K. *Appl. Surf. Sci.* **1997**, *110*, 616.
(9) Chen, S.; Grigoropoulos, C. P. *Appl. Phys. Lett.* **1997**, *71*, 3191.
(10) Nettesheim, S.; Zenobi, R. *Chem. Phys. Lett.* **1996**, *255*, 39.
(11) Sadeghi, M.; Vertes, A. *Appl. Surf. Sci.* **1998**, *127*, 226.
(12) Stevenson, E.; Breuker, K.; Zenobi, R. *J. Mass Spectrom.* **2000**, *35*, 1035.
(13) Harmer, J. D.; Watts, B. N. *J. Sci. Instrum.* **1955**, *32*, 167.
(14) Wieting, T. J.; Schriempf, J. T. *J. Appl. Phys.* **1976**, *47*, 4009.
(15) Gay, F. P. *J. Polym. Sci., Part B: Polym. Phys.* **1973**, *11*, 2227.
(16) *Theory and Practice of Radiation Thermometry*; Dewitt, D. P., Nutter, G. D., Eds.; Wiley: New York, 1988.
(17) Kanstad, S. O.; Nordal, P.-E. *Can. J. Phys.* **1986**, *64*, 1155.
(18) In *Thermal Radiative Heat Transfer*, 3rd ed.; Siegel, R., Howell, J. R., Eds.; Hemisphere: Bristle, 1992.
(19) Allwood, D. A.; Dyer, P. E. *Chem. Phys.* **2000**, *261*, 457.
(20) Vertes, A.; Gijbels, R.; Levine, R. D. *Rapid Commun. Mass Spectrom.* **1990**, *4*, 228.